Annals of Botany **132**: 1205–1217, 2023
https://doi.org/10.1093/aob/mcad164, available online at www.academic.oup.com/aob

ANNALS OF BOTANY
Founded 1887

Spatio-temporal expression of candidate genes for nectar spur development in *Tropaeolum* (Tropaeolaceae: Brassicales)

Sebastián Martínez-Salazar[1,2], Elena M. Kramer[2], Favio González[3] and Natalia Pabón-Mora[1,*]

[1]Instituto de Biología, Universidad de Antioquia, Medellín 050010, Colombia, [2]Department of Organismic and Evolutionary Biology, Harvard University, Cambridge, MA 02138, USA, and [3]Universidad Nacional de Colombia, Facultad de Ciencias, Instituto de Ciencias Naturales, Sede Bogotá 111321, Colombia
[*]For correspondence. E-mail lucia.pabon@udea.edu.co

Received: 30 June 2023 Returned for revision: 30 August 2023 Editorial decision: 12 October 2023 Accepted: 16 October 2023

• **Background and Aims:** Tropaeolaceae (Brassicales) comprise ~100 species native to South and Central America. Tropaeolaceae flowers have a nectar spur, formed by a late expansion and evagination of the fused proximal region of the perianth (i.e. the floral tube). This spur is formed in the domain of the tube oriented towards the inflorescence axis, which corresponds to the adaxial floral region. However, little is known about the molecular mechanisms responsible for the evolution of spurs in Tropaeolaceae.
• **Methods:** In this study, we examined the spatio-temporal expression of genes putatively responsible for differential patterns of cell division between the adaxial and abaxial floral regions in Tropaeolaceae. These genes include previously identified *TCP* and *KNOX* transcription factors and the cell division marker *HISTONE H4* (*HIS4*).
• **Key Results:** We found a *TCP4* homologue concomitantly expressed with spur initiation and elaboration. Tropaeolaceae possess two *TCP4-like* (*TCP4L*) copies, as a result of a Tropaeolaceae-specific duplication. The two copies (*TCP4L1* and *TCP4L2*) in *Tropaeolum longifolium* show overlapping expression in the epidermis of reproductive apices (inflorescence meristems) and young floral buds, but only *TlTCP4L2* shows differential expression in the floral tube at early stages of spur formation, restricted to the adaxial region. This adaxial expression of *TlTCP4L2* overlaps with the expression of *TlHIS4*. Later in development, only *TlTCP4L2* is expressed in the nectariferous tissue of the spur.
• **Conclusions:** Based on these results, we hypothesize that Tropaeolaceae *TCP4L* genes had a plesiomorphic role in epidermal development and that, after gene duplication, *TCP4L2* acquired a new function in spur initiation and elaboration. To better understand spur evolution in Tropaeolaceae, it is critical to expand developmental genetic studies to their sister group, the Akaniaceae, which possess simultaneously an independent duplication of *TCP4L* genes and a spurless floral tube.

Key words: Brassicales, *CINCINNATA*, evo-devo, *HISTONE H4*, *KNOXI*, spur evolution, *TCP*, *Tropaeolum*.

INTRODUCTION

Nectar spurs are tubular outgrowths, derived from flowers, that produce or accumulate nectar. They have evolved several times from spurless lineages across angiosperms, likely playing key roles in establishing plant–pollinator interactions (Hodges and Arnold, 1995; Hodges, 1997; Vlašánková *et al*., 2017). A nectar spur is a synapomorphy of the Tropaeolaceae (nasturtiums), which comprise the single genus *Tropaeolum* with ~100 species (Andersson and Andersson, 2000). Tropaeolaceae corresponds to the only example of spur evolution in the order Brassicales, to which the model *Arabidopsis thaliana* belongs. In particular, spurs in Tropaeolaceae are derived from one side of the proximal perianth floral tube (Fig. 1). Flowers in Tropaeolaceae are axillary, with one domain towards the shoot apical meristem and another one away from it [hereafter called the adaxial and the abaxial region, respectively equivalent to the dorsal and ventral region commonly used in Plantaginaceae literature (since Luo *et al*., 1996)] (Fig. 1A–G). Additionally, the Tropaeolaceae floral tube itself has surfaces closer to or away from the flower meristem, which we will respectively refer to as the inner and outer surfaces, rather than the adaxial and abaxial surfaces, for clarity (Fig. 1H–I). After all five sepal and five petal primordia are initiated, the adaxial region of the floral tube expands and evaginates, forming the spur, resulting in a bilaterally symmetrical flower (Martínez-Salazar *et al*., 2021). Consequently, the three adaxial sepals and the two adaxial petals are inserted at the opening of the spur (Ronse De Craene and Smets, 2001; Martínez-Salazar *et al*., 2021). In contrast, Akaniaceae, the sister group of Tropaeolaceae, have a spurless floral tube. The floral tube (also called the cup) in Akaniaceae lifts all five sepals and five petals, but does not exhibit adaxial–abaxial differential growth, so remains radially symmetrical (Ronse De Craene *et al*., 2002). Therefore, understanding genetic differences between the adaxial and abaxial regions of the floral tube in Tropaeolaceae could shed light on the mechanisms recruited for spur development and evolution in this lineage.

Molecular mechanisms responsible for nectar spur development can be directly or indirectly linked to the dynamics of cell division and differentiation in floral tissues (Dupuy *et*

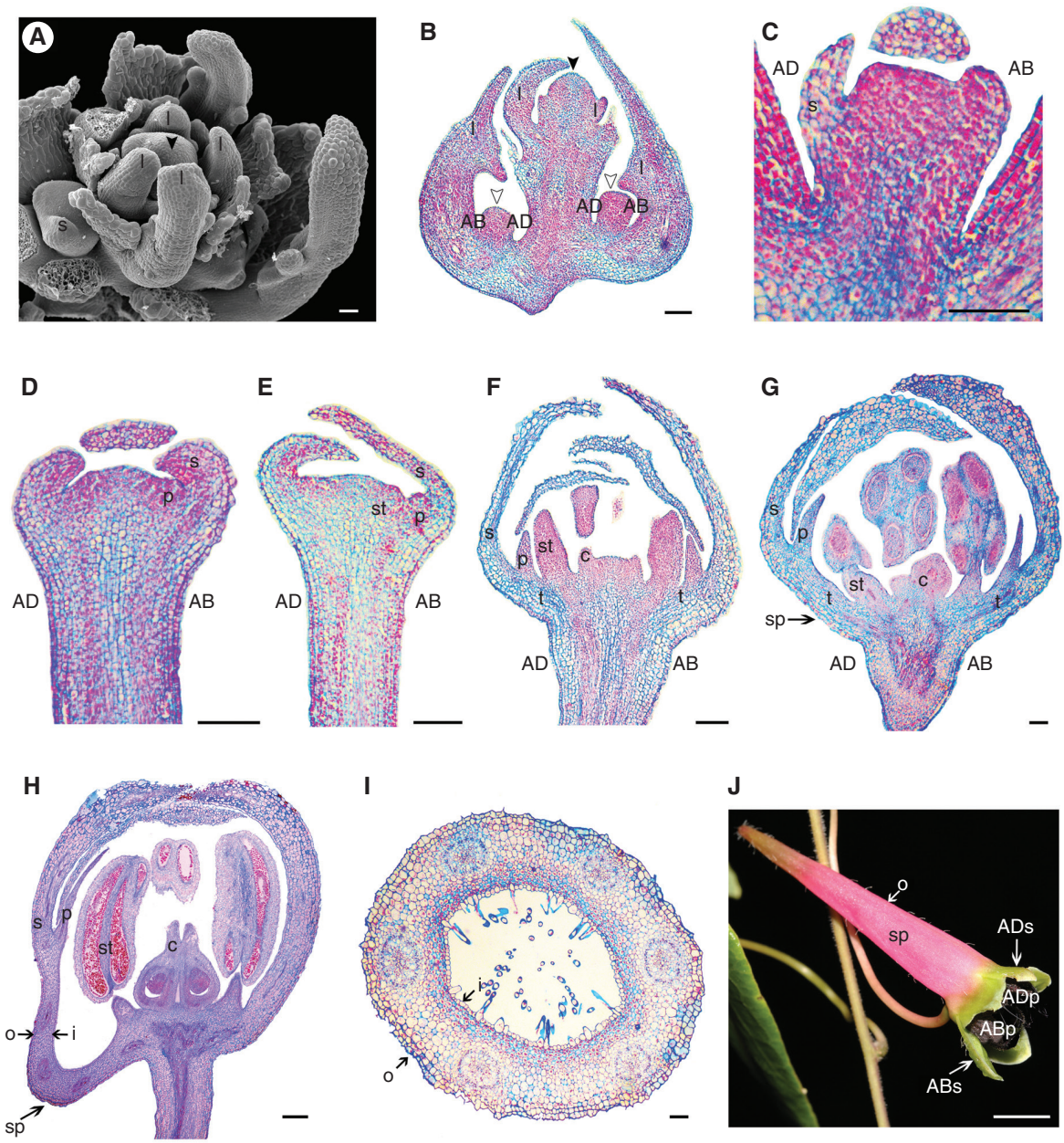

FIG. 1. Flower developmental stages of *Tropaeolum longifolium*. (A, B) Flowering shoot apex as seen by scanning electron microscopy (A) and light microscopy (B, longitudinal section). (C–H) Longitudinal sections of flowers at S1 (C), S2 (D), S3 (E), S4 (F), S5 (G) and S6 (H). (I) Transverse section of the nectariferous region of the spur at S8. (J) Flower in anthesis. Sections in B–I are stained with safranin and astra blue. AB, abaxial region of the flower; ABp, abaxial petal; ABs, abaxial sepal; AD, adaxial region of the flower; ADp, adaxial petal; AD, adaxial sepal; c, carpel; i, inner surface of the floral tube; l, leaf; o, outer surface of the floral tube; p, petal; s, sepal; sp, spur; st, stamen; t, floral tube. Black arrowheads point to the shoot apical meristem; white arrowheads point to floral primordia. Scale bars: A–G, I = 50 µm; H = 500 µm; J = 1 cm.

al., 2010; Rebocho *et al.*, 2017). In plants such as *Aquilegia*, *Epimedium* and *Halenia*, spurs are formed homogeneously in all petals without altering the floral radial symmetry. The genetic regulation of spur formation is better known in *Aquilegia* (Ranunculaceae), where the *C2H2* zinc-finger transcription factor *POPOVICH* (*POP*) promotes cell division in petals. Consequently, downregulation of *POP* reduces or completely suppresses spur development (Ballerini *et al.*, 2020). Additionally, other transcription factors inhibit cell division in *Aquilegia* spurs, sculpting their final shape. This is the case for the class II *TCP* (*TEOSINTE BRANCHED1*, *CYCLOIDEA*, and *PROLIFERATING CELL FACTOR*) gene *AqTCP4*. Downregulation of *AqTCP4* produces ectopic outgrowths in the distal surface of the spur (Yant *et al.*, 2015).

In other plants, spurs are produced by differentially regulating tissue growth in the floral meristem, forming bilaterally symmetrical flowers (e.g. *Delphinium*, *Linaria* and Tropaeolaceae). In *Linaria* (Plantaginaceae), only the ventral petal produces a spur. However, the genetic mechanisms recruited for dorsal–ventral differential growth have been better investigated in the

closely related *Antirrhinum majus*. In this species, bilateral symmetry is regulated by the class II *TCP* transcription factors *CYCLOIDEA* (*CYC*) and *DICHOTOMA* (*DICH*) (Luo *et al*., 1996), and the *MYB* (*Myeloblastosis*) transcription factors *RADIALIS* (*RAD*) and *DIVARICATA* (*DIV*) (Almeida *et al*., 1997; Corley *et al*., 2005). *CYC* and *DICH* activate *RAD* in the dorsal region of the flower, which regulates tissue growth and restricts *DIV* activity to the ventral region. When the orthologue of *CYC* in *Linaria* is silenced, all five petals produce spurs (Cubas *et al*., 1999*b*). Additionally, in *Antirrhinum*, ectopic expression of the class I *KNOX* (*KNOTTED1-LIKE HOMEOBOX*) transcription factor *HIRZINA* (*HIRZ*) or *INVAGINATA* (*INA*) produces a tubular outgrowth in the ventral petal (Golz *et al*., 2002). The orthologues of *HIRZ* and *INA* in *Linaria* are expressed in the spur and their heterologous overexpression in *Nicotiana* can induce sac-like outgrowths in petals (Box *et al*., 2011).

In a previous study using RT–PCR, we examined the expression of homologues of all the above-mentioned transcription factors in *Tropaeolum longifolium*, specifically comparing the adaxial and abaxial regions of the floral tube at late stages of development (Martínez-Salazar *et al*., 2021). Our hypothesis was that some of them could have been recruited downstream of floral symmetry to regulate tissue growth in the adaxial region of the floral tube forming the spur. In fact, we found that *TlTCP4L2*, a class II *TCP* homologue from the *CINCINNATA3* (*CIN3*) lineage, is exclusively expressed in the adaxial region. Conversely, *TlTCP12*, a class II *TCP* homologue from the *CYCLOIDEA3* (*CYC3*) lineage, and *TlSTM1*, a class I *KNOX* gene from the *SHOOT MERISTEMLESS* (*STM*) lineage, are exclusively expressed in the spurless abaxial region of the floral tube. The closest paralogues of *TlTCP4L2* and *TlSTM1* (*TlTCP4L1* and *TlSTM2*, respectively) are expressed homogenously throughout the floral tube. However, the expression patterns of all of these genes at earlier stages of flower development when the spur initiates and their correlation with cell division dynamics in the floral tube remain unknown. Additionally, it is unclear if their expression patterns are exclusive to the floral tube or if they expand to broader domains of the flower.

Here, we aimed to examine in detail the spatio-temporal expression patterns of *TlTCP4L1*, *TlTCP4L2*, *TlTCP12*, *TlSTM1* and *TlSTM2* in *T. longifolium* flowers using RNA *in situ* hybridization to better characterize their putative role in spur development. In addition, we analysed the expression of *TlHIS4* as a marker of cell division to test whether the onset of differential cell division in the floral tube of *T. longifolium* is linked to spur formation.

MATERIALS AND METHODS

We localized the mRNA of our genes of interest in sectioned flowers of *Tropaeolum longifolium* Turcz. (*Tl*) at different stages of development (Fig. 1). These genes are *TlTCP4L1* and *TlTCP4L2* (*CINCINNATA* homologues); *TlTCP12* (a *CYCLOIDEA3* homologue); *TlSTM1* and *TlSTM2* (*SHOOT MERISTEMLESS* homologues); and finally *TlHIS4* (*HISTONE H4* as a cell division marker). Steps for mRNA localization included tissue fixation, total RNA extraction, primer design, template DNA synthesis, RNA probe synthesis and *in situ* hybridization.

Tissue fixation

To obtain fixed tissue samples, we collected reproductive apices and flowers at stages S0–S8 (as defined by Martínez-Salazar *et al*., 2021) of *T. longifolium* (Fig. 1) in cold, freshly prepared FAA (3.7% formaldehyde, 5% acetic acid and 50% ethyl alcohol). We dehydrated these samples in a series of ethanol–HistoChoice, embedded them in Paraplast X-tra (Leica Biosystems, Richmond, IL, USA) and stored them at 4 °C until use.

Total RNA extraction

To obtain total RNA for cDNA synthesis, we collected reproductive apices of *T. longifolium* and flash-froze them in liquid nitrogen. We extracted total RNA from collected apices, using TRIsure (Bioline, Memphis, TN, USA), and quantified it using a NanoDrop 2000 spectrophotometer (Thermo Scientific, Waltham, MA, USA). We treated total RNA with RQ1 RNase-Free DNase (Promega, Madison, WI, USA) and stored it at −80 °C until use.

Primer design

To amplify DNA templates for anti-sense RNA probe synthesis, we designed primers for our genes of interest (Supplementary Data Table S1). We designed primers targeting gene-specific sequences of 250–550 bp and avoiding conserved regions between paralogues. We included the T7 RNA polymerase promoter sequence (5′ CTTAATACGACTCACTATAGGG 3′) at the 5′ end of each reverse primer. As a negative control for *in situ* hybridization, we designed primers to synthesize a sense probe for *TlHIS4*, including the T7 promoter sequence at the 5′ end of the forward primer.

Template DNA synthesis

We obtained DNA templates for RNA probe synthesis using a two-step RT–PCR. For the first step of the RT–PCR, we used 3 µg of DNase-treated total RNA as a template to synthesize cDNA using SuperScript® III Reverse Transcriptase (Invitrogen) and oligo dT primers. For the second step, we did a specific amplification reaction for each gene of interest as follows. We made master mixes of 50 µL of EconoTaq DNA Polymerase (Lucigen, Middleton, WI, USA), 31 µL of nuclease-free water, 5 µL of betaine (5 µg mL^{-1}), 5 µL of bovine serum albumin (5 µg mL^{-1}), 3 µL of each forward and reverse primer (10 mM), and 3 µL of cDNA, for a total reaction volume of 100 µL each. We subjected each mix to an initial denaturation step (94 °C for 4 min); 36 cycles of denaturation (94 °C for 30 s), annealing (49–61 °C depending on the primer combination, for 30 s) and extension (72 °C for 50 s); and a final extension step (72 °C for 10 min). We purified the resulting amplicons using the PureLink® PCR Purification Kit (Invitrogen). We quantified the

purified amplicons using a Multiskan Sky spectrophotometer (Thermo Scientific) and stored them at −20 °C until use.

RNA probe synthesis

We synthesized digoxigenin (DIG)-labelled RNA probes for each of our genes of interest. We used 1–2 µg of each purified amplicon as a template to synthesize its corresponding probe using T7 RNA Polymerase (Roche, Basel, Switzerland) and DIG RNA Labeling Mix (Roche). We treated resulting probes with RQ1 RNase-Free DNase (Promega) and ran them in a 1 % agarose gel to compare them with DNA templates (Supplementary Data Fig. S1). We precipitated DNase-treated probes using 62.5 µL of absolute ethanol, 2.5 µL of 3 M sodium acetate (pH = 5.2) and 1 µL of 10 mg mL^{-1} yeast tRNA, and stored them over 1 d at −20 °C until centrifugation. We centrifuged precipitated probes, washed them with ethanol and resuspended them in hybridization buffer (50% formamide, 3% SDS, 6× SSC and 100 µg mL^{-1} yeast tRNA). We stored resuspended probes at room temperature until use.

In situ hybridization

We performed RNA *in situ* hybridization in fixed *T. longifolium* samples using the probes we synthesized for our genes of interest. We sectioned fixed samples on a Leica RM2125 RTS rotary microtome to 10 µm thickness. The *in situ* hybridization procedure on sectioned samples followed Ferrándiz *et al.* (2000). Whenever possible, we hybridized consecutive sections of the same floral bud with either *TlHIS4* or *TlTCP4L2* anti-sense probes. In parallel, we prepared standard sections stained with safranin and astra blue as a reference to compare with hybridized samples. We dehydrated resulting slides, mounted them in Entellan (Merck, Darmstadt, Germany) and visualized them under a Leica DM500 optical microscope equipped with a Leica ICC50W camera to photograph them using LAS EZ software.

Phylogenetic analyses

In addition to characterizing spatio-temporal expression patterns of our genes of interest, we aimed to infer if the duplications that gave rise to Tropaeolaceae *TCP4L1/2* and *STM1/2* occurred before or after the Akaniaceae–Tropaeolaceae divergence. To do so, we isolated homologous sequences of *CIN3* (*TCP10* and *TCP3/4L*) and *STM* genes from the recently assembled genomes of *Bretschneidera sinensis* (Akaniaceae), based on the annotation provided (Liu *et al*., 2022; Zhang *et al*., 2022). We compiled these sequences with orthologues from Tropaeolaceae and other angiosperms, downloaded from our own generated transcriptomes (Martínez-Salazar *et al*., 2021) and publicly available databases: Phytozome (https://phytozome-next.jgi.doe.gov/), GenBank (https://www.ncbi.nlm.nih.gov/genbank/) and 1KP (https://db.cngb.org/onekp/) in one matrix per gene family (Supplementary Data Table S2). To infer positional homology, we aligned each matrix using MAFFT in the TranslatorX server (http://translatorx.co.uk/; Abascal *et al*., 2010). We submitted each aligned matrix to a maximum likelihood analysis using raxmlGUI 1.5 beta (Silvestro and Michalak, 2012) with 1000 bootstrap repetitions, a Generalized time-reversible (GTR) substitution model, and additional default settings. We visualized and edited phylogenetic trees in the Interactive Tree Of Life (iTOL) (Letunic and Bork, 2019).

RESULTS

Our goal was to identify the spatio-temporal expression patterns of transcription factors putatively involved in establishing differential growth patterns between the adaxial (spur-bearing) and abaxial (spur-lacking) floral regions of *T. longifolium* (Fig. 1; Martínez-Salazar *et al*., 2021). We examined expression patterns in inflorescence meristems with young floral primordia (stage 0; Fig. 1A, B), floral buds with sepals developed (stage 1; Fig. 1C), floral buds with petals developed (stage 2; Fig. 1D), floral buds with stamens developed (stage 3; Fig. 1E), floral buds with carpels developed (stage 4; Fig. 1F), floral buds at spur initiation (stage 5; Fig. 1G), during early spur elongation (stage 6; Fig. 1H), and fully formed spurs having an inner nectariferous tissue with large nuclei and trichomes (Fig. 1I). Henceforth, we will first describe the cell division patterns leading to spur growth using *HISTONE4*, then we describe expression patterns of the genes that likely contribute to differential growth in the floral tube, and finally we report the genes that do not show differential adaxial–abaxial expression during spur formation or elongation.

Expression of the cell division marker *Tropaeolum longifolium HISTONE H4 (TlHIS4)*

In order to understand the dynamics of cell division during floral development and in the floral tube, we tested the expression of the *HISTONE H4* homologue *TlHIS4*. *TlHIS4* expression can be detected in the shoot apical meristem (especially in the central zone), young leaves, stems and flower primordia at different developmental stages (Fig. 2A, B). At early stages of flower development (S1–S3), expression of this gene is concentrated in developing sepals, petals, stamens and carpels, as well as in the flower pedicel, without differential expression between the adaxial and abaxial regions of the floral tube (Fig. 2C, D). At stage S5, when the spur initiates, *TlHIS4* expression is concentrated in the adaxial region of the floral tube (Fig. 2E). At this stage, *TlHIS4* continues to be expressed in petals, stamens, carpels and ovule primordia. At S6 and S7, when the spur elongates, *TlHIS4* maintains its expression in the adaxial region of the floral tube, petals, stamens, carpels and ovules (Fig. 2F–K). The expression of *TlHIS4* at S6 in the spur is more evident in the outer epidermal and subepidermal layers (Fig. 2F, G, I). At later stages of flower development (S8), *TlHIS4* is expressed in the inner layers of the spur, where the nectariferous tissue is located (Fig. 2L).

Evolution and expression of the *CINCINNATA3* homologues *TlTCP4L1* and *TlTCP4L2*

To have a phylogenetic framework for *TlTCP4L1* and *TlTCP4L2*, we first reconstructed the evolutionary relationships of different Brassicales *CIN3* homologues (Fig. 3).

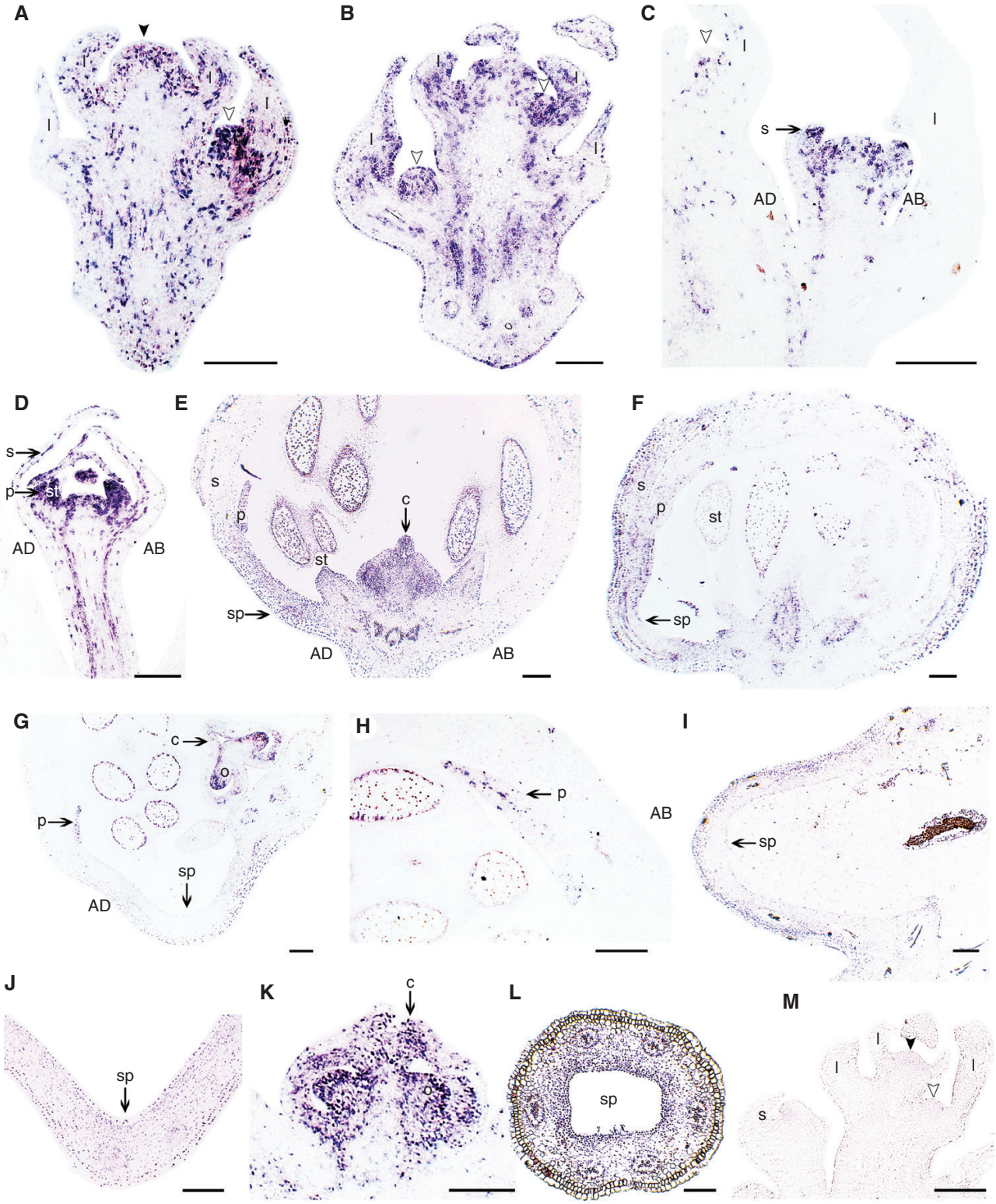

FIG. 2. Expression of *Tropaeolum longifolium HISTONE H4* (*TlHIS4*) using *in situ* hybridization. (A, B) Longitudinal section through a shoot apex, showing axillary floral primordia. (C, D) Longitudinal section of flowers at S0 and S1 (C), and S3 (D). (E) Longitudinal section of a flower at S5, showing spur initiation in the adaxial region. (F) Longitudinal section of a flower at S6. (G, H) Detail of the adaxial (G) and abaxial (H) regions of the floral tube at S6, during early spur elongation. (I) Longitudinal section of the spur at S6. (J) Detail of the spur during elongation at S7. (K) Longitudinal section of carpels with ovules. (L) Transverse section of the nectariferous region of the spur at S8. (M) Longitudinal section through a shoot apex hybridized with a sense probe. AB, abaxial region of the flower; AD, adaxial region of the flower; c, carpel; l, leaf; o, ovule; p, petal; s, sepal; sp, spur; st, stamen. Black arrowheads point to shoot apical meristems; white arrowheads point to floral primordia. Scale bars = 200 μm.

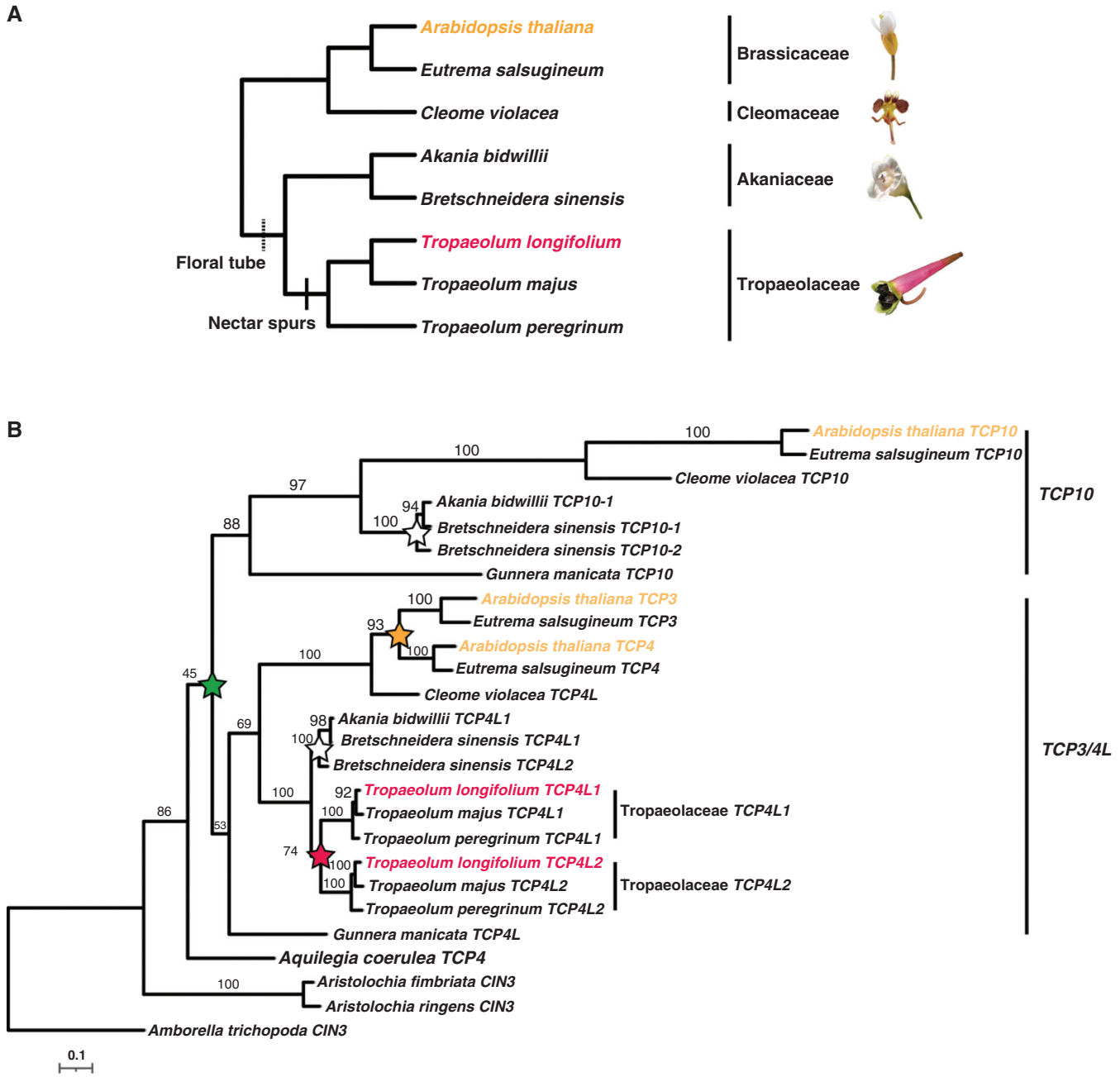

FIG. 3. Evolution of *CINCINNATA3* genes. (A) Schematic phylogenetic relationships of the Brassicales species used in the analysis. Mapping of the nectar spur and presumed floral tube evolution are marked on the tree. Photographs of a representative of each family are shown as follows: *Arabidopsis thaliana* for Brassicaceae; *Cleome violacea* for Cleomaceae (photograph taken and modified from iNaturalist © Lies Van Rompaey); *Bretschneidera sinensis* for Akaniaceae; and *Tropaeolum longifolium* for Tropaeolaceae. (B) Maximum likelihood analysis of *CIN3* genes. Gene duplication events are indicated with stars: green star, duplication predating core eudicot diversification; orange star, duplication predating Brassicaceae diversification; white stars, duplications predating Akaniaceae diversification; red star, duplication predating Tropaeolaceae diversification. Names in orange correspond to *A. thaliana* canonical homologues; names in red correspond to the *T. longifolium* homologues *TlTCP4L1* and *TlTCP4L2*. Node numbers indicate bootstrap support.

Our sampling included two Brassicaceae, one Cleomaceae, two Akaniaceae and three Tropaeolaceae species (Fig. 3A), as well as some angiosperm outgroups. We retrieved a duplication specific to core eudicots, which gave rise to the clades *TCP3/4L* and *TCP10* (Fig. 3B). Genes from the *TCP3/4L* clade underwent independent duplications in Brassicaceae, giving rise to *TCP3* and *TCP4*; Akaniaceae, giving rise to the Akaniaceae-specific *TCP4L1* and *TCP4L2*; and Tropaeolaceae, giving rise to the Tropaeolaceae-specific *TCP4L1* and *TCP4L2*, which includes *TlTCP4L1* and *TlTCP4L2*. We did not find *TCP10* orthologues in Tropaeolaceae.

TlTCP4L1 and *TlTCP4L2* have distinctive expression in the epidermal layer of the reproductive apex, including the shoot

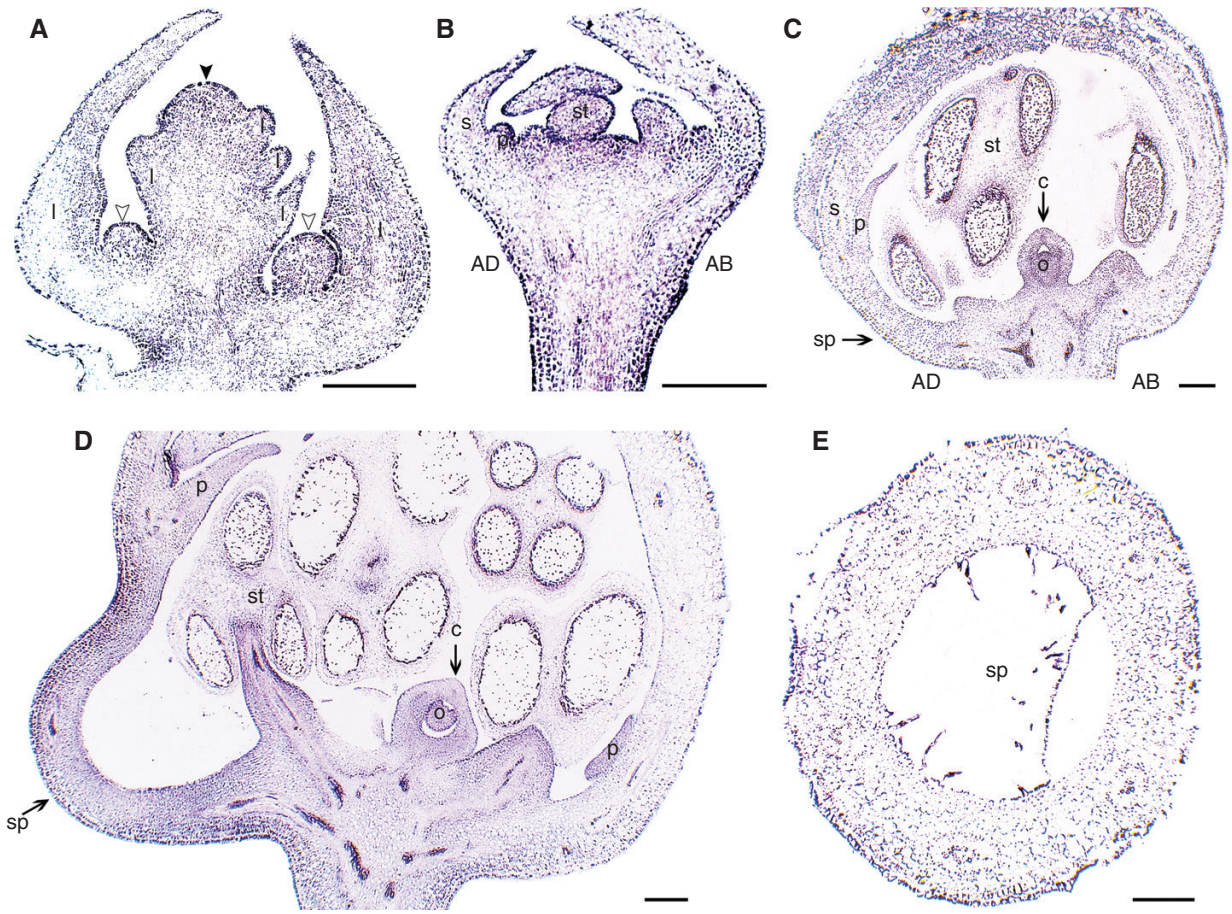

FIG. 4. Expression of *Tropaeolum longifolium TlTCP4L1* using *in situ* hybridization. (A) Longitudinal section through a shoot apex, showing axillary floral primordia. (B) Longitudinal section of a flower at S3. (C) Longitudinal section of a flower at S5, showing spur initiation in the adaxial region. (D) Longitudinal section of a flower at S6 at early spur elongation. (E) Transverse section of the nectariferous region of the spur at S8. AB, abaxial region of the flower; AD, adaxial region of the flower; c, carpel; l, leaf; o, ovule; p, petal; s, sepal; sp, spur; st, stamen. Black arrowhead points to the shoot apical meristem; white arrowheads point to floral primordia. Scale bars = 200 μm.

apical meristem, leaf primordia, stems and floral primordia prior to sepal initiation (Figs 4A and 5A, B). The epidermal expression is maintained in flowers at S3 and S4, when the two genes are strongly expressed in the epidermis and the two or three subepidermal layers of sepals, petals, stamens and the flower pedicel (Figs 4B and 5C, D). At S3 and S4, no obvious differential expression between the adaxial and abaxial regions of the floral tube is detected for *TlTCP4L1* or *TlTCP4L2* (Figs 4B and 5C, D). At S5 (spur initiation), the expression patterns of the two paralogues begin to diverge. *TlTCP4L1* is predominantly expressed in the epidermal layer of the floral tube, with an overall weak expression in the adaxial region (Fig. 4C). Conversely, *TlTCP4L2* expression at S5 is much higher in the adaxial region of the floral tube (Fig. 5E–I), overlapping with the expression of *TlHIS4* (Fig. 2E). Additionally, the two paralogues are strongly expressed in petals, filaments, carpels and ovules.

At S6, when the spur begins to elongate, the expression of *TlTCP4L1* and *TlTCP4L2* can be detected more strongly in the adaxial region of the floral tube, petals, filaments, carpels and ovules (Figs 4D and 5J, K). This adaxially localized expression is more evident for *TlTCP4L2*, which has expanded its expression throughout the spur (Fig. 5J, K) compared with earlier developmental stages (Fig. 5H, I). The expression of *TlTCP4L2* in carpels is stronger in epidermal layers, including the inner and outer epidermis of the carpel wall and the epidermis of developing ovules (Fig. 5L).

At later stages (S8), *TlTCP4L1* maintains its expression in the inner and outer epidermis of the floral tube, including the spur (Fig. 4E). Conversely, *TlTCP4L2* is strongly expressed in the inner portion of the spur, where the nectariferous tissue is located (Fig. 5M). This gene is also expressed in the phloem of the amphicribal vascular bundles that run through the spur. However, *TlTCP4L2* is not expressed in the layer of parenchyma cells located between the phloem and the inner nectariferous tissue (Fig. 5M).

Expression of transcription factor *TlTCP12*

Previous studies by RT–PCR had suggested that *TlTCP12* was specifically expressed in the spurless abaxial region of the *T. longifolium* flower at late stages of development (Martínez-Salazar *et al.*, 2021). Detailed *in situ* hybridization shows that *TlTCP12* is expressed in the shoot apical meristem, as

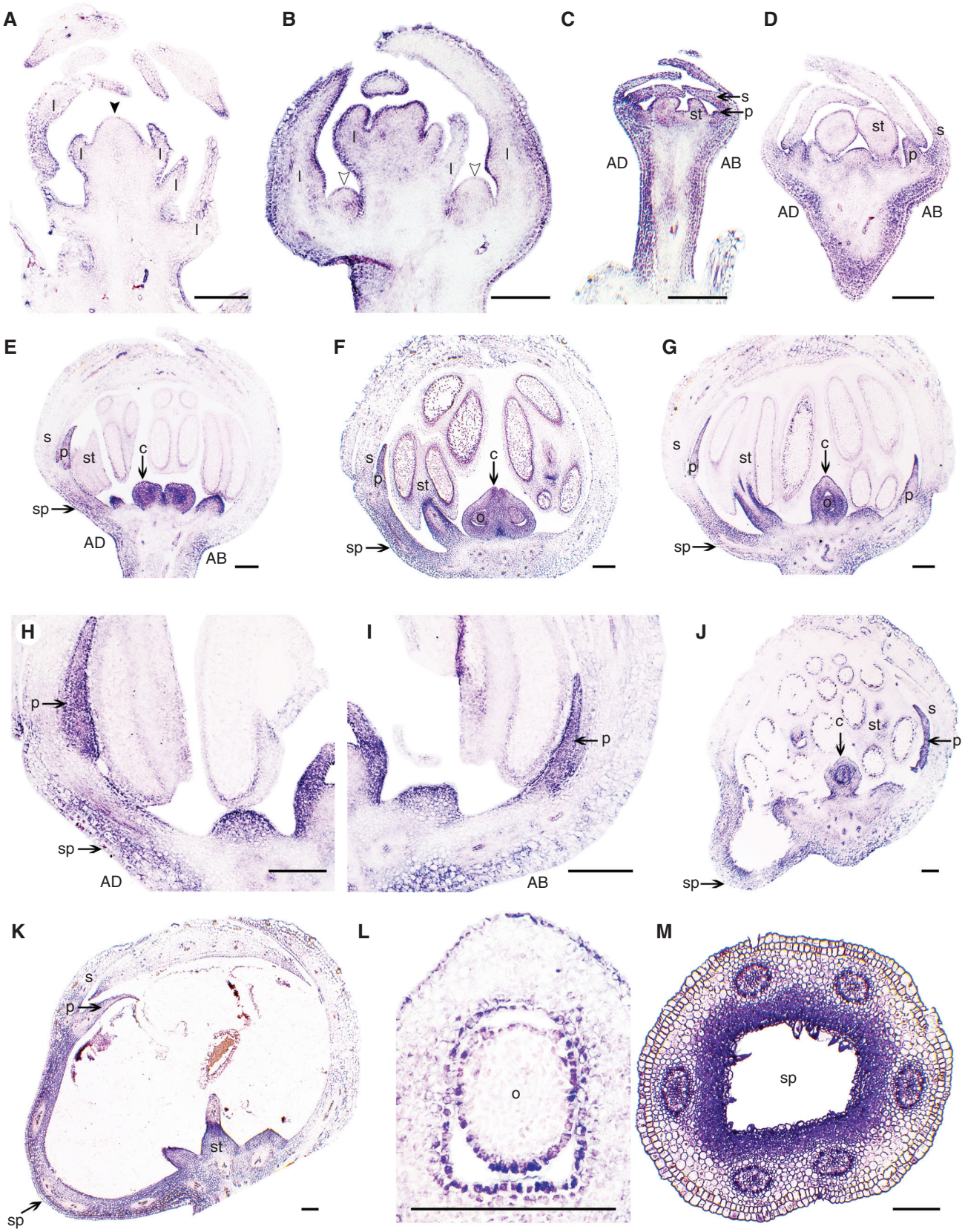

FIG. 5. Expression of *Tropaeolum longifolium TlTCP4L2* using *in situ* hybridization. (A, B) Longitudinal sections through a shoot apex; note two axillary floral primordia (B). (C, D) Longitudinal section of flowers at S3 (C) and S4 (D). (E–G) Longitudinal sections of flowers at S5, showing spur initiation in the adaxial region. (H, I) Detail of adaxial (H) and abaxial (I) regions of the floral tube at S5. (J, K) Longitudinal section of flowers at S6 during early spur elongation. (L) Transverse section of one of the three carpels with one ovule. (M) Transverse section of the nectariferous region of the spur at S8. AB, abaxial region of the flower; AD, adaxial region of the flower; c, carpel; l, leaf; o, ovule; p, petal; s, sepal; sp, spur; st, stamen. Black arrowhead points to the shoot apical meristem; white arrowheads point to floral primordia. Scale bars = 200 μm.

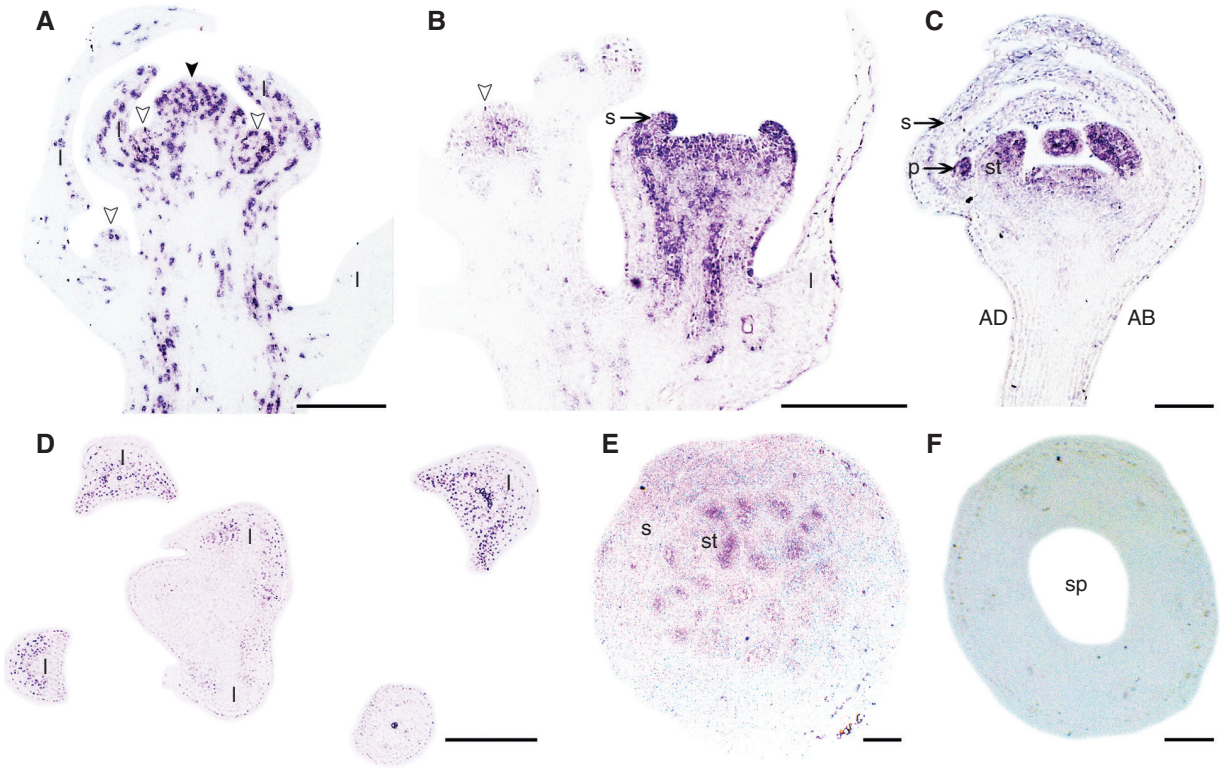

FIG. 6. Expression of *Tropaeolum longifolium TlTCP12* using *in situ* hybridization. (A) Longitudinal section through a shoot apex, showing axillary floral primordia. (B, C) Longitudinal section of floral buds at S0 and S1 (B), and S3 (C). (D) Transverse section of the shoot apex. (E) Transverse section of a flower at S5. (F) Transverse section through the nectariferous region of the spur at S8. AB, abaxial region of the flower; AD, adaxial region of the flower; l, leaf; p, petal; s, sepal; sp, spur; st, stamen. Black arrowhead points to the shoot apical meristems; white arrowheads point to floral primordia. Scale bars = 200 µm.

well as in leaf and floral primordia (Fig. 6A, D). At stage S1, *TlTCP12* is expressed in sepal tips, flower vasculature and the centre of the flower (Fig. 6B). At S3, the expression of this gene is restricted to petals, stamens and developing carpels (Fig. 6C). At later stages of development, the expression of *TlTCP12* is barely detected (Fig. 6E) and does not occur in the spur (Fig. 6F). Overall, we did not detect differential expression of this gene between the adaxial and abaxial regions of the floral tube.

Expression of transcription factors *TlSTM1* and *TlSTM2*

In addition to *TlTCP12*, previous analyses by RT–PCR had suggested that at least one of the *SHOOT MERISTEMLESS* homologues in *T. longifolium* was also specifically expressed at late developmental stages in the abaxial spurless region of the floral tube (Martínez-Salazar *et al.*, 2021). Thus, we tested the spatio-temporal expression of *TlSTM1* and its closest paralogue, *TlSTM2*. These genes are the result of a duplication that occurred after the Akaniaceae–Tropaeolaceae divergence (Supplementary Data Fig. S2). Our results show that *TlSTM1* and *TlSTM2* have similar scattered expression patterns in the shoot apical meristem (Fig. 7A, H). Transcripts of the two genes are detected in leaves, albeit poorly, throughout their development (Fig. 7A, H). Both genes have an increased expression in floral meristems compared with the shoot apical meristem (Fig. 7A–C, H). These genes are expressed at S1 in young sepals and in the central dome of the flower, where petals, stamens and carpels will be formed (Fig. 7D, H). At S4, their expression is restricted to the differentiating carpellary tissue at the centre of the flower (Fig. 7E, I). At stage S5, *TlSTM1* expression is restricted to receptacle vasculature, carpels and ovules (Fig. 7F, G), whereas *TlSTM2* expression is no longer detected (Fig. 7J). Remarkably, we did not detect strong expression of these genes in the floral tube.

DISCUSSION

TlTCP4L1 and *TlTCP4L2* expression patterns suggest neofunctionalization after gene duplication

We described divergent expression patterns for the paralogues *TlTCP4L1* and *TlTCP4L2*. Both paralogues are highly expressed in the epidermis of reproductive apices, flower meristems and flower organ primordia (Figs 4A, B and 5A–D). However, only *TlTCP4L2* is strongly expressed in the nascent spur right before evagination (Figs 4C and 5E–H), while both genes regain high overlapping expression during spur growth (Figs 4D and 5J, K). In fully developed spurs, *TlTCP4L1* is continuously expressed in the inner and outer epidermis (Fig. 4E), whereas *TlTCP4L2* is expressed in the nectariferous tissue (Fig. 5M). These results suggest that the Tropaeolaceae *TCP4L2* gene copy might have acquired a role in spur initiation and nectary development after gene duplication, concordant

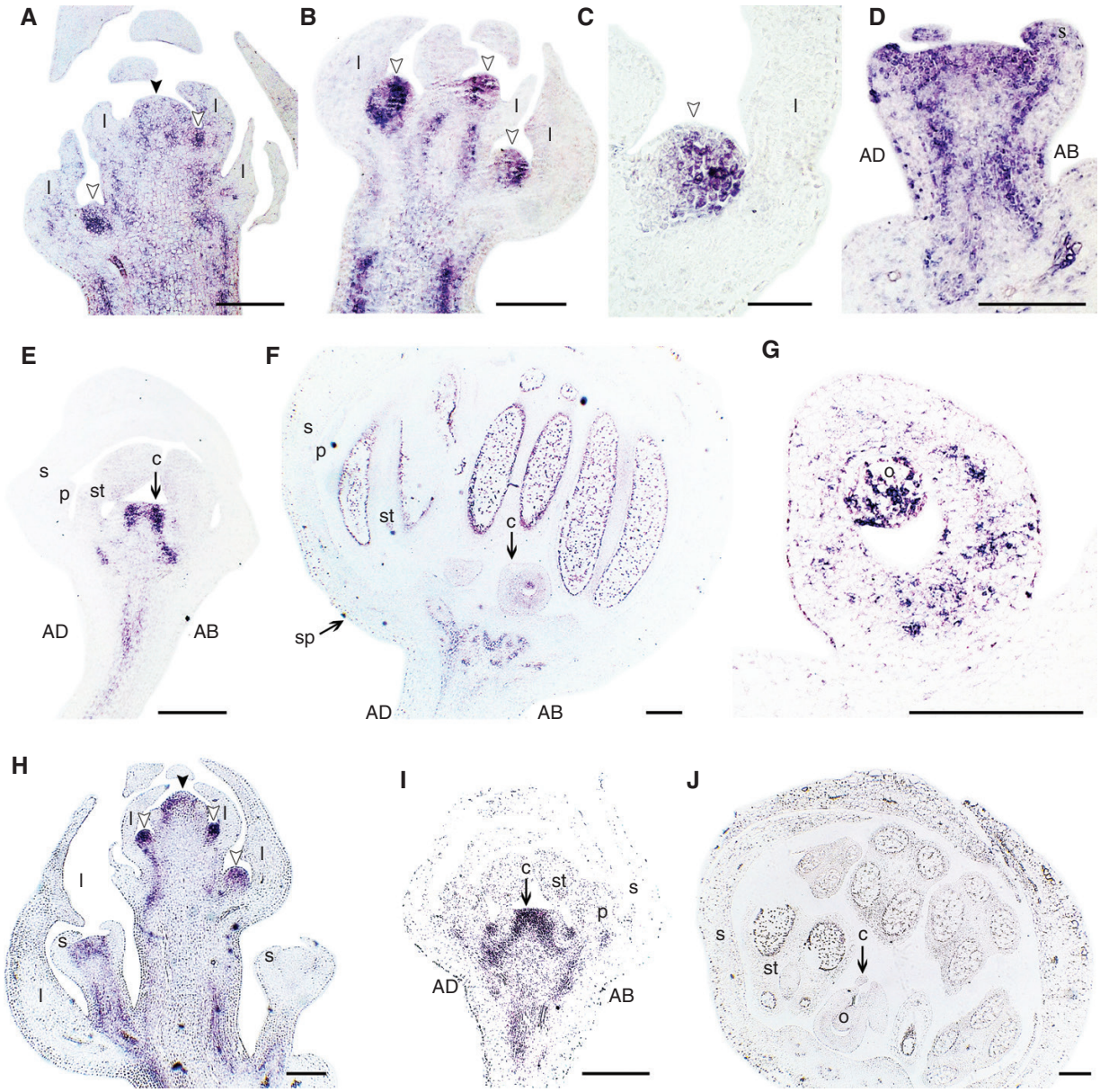

FIG. 7. Expression of *Tropaeolum longifolium SHOOT MERISTEMLESS1/2*, *TlSTM1* (A–G) and *TlSTM2* (H–J) using *in situ* hybridization. (A) Longitudinal section through the shoot apex and axillary floral primordia. (B) Detail of axillary floral meristems. (C–E) Longitudinal section of flowers at S0 (C), S1 (D) and S4 (E). (F) Longitudinal section of a flower at S5, showing spur initiation in the adaxial region. (G) Longitudinal section of one of the three carpels with an ovule. (H) Longitudinal section through the shoot apical meristem, showing axillary floral primordia at stages S0 and S1. (I) Longitudinal section of a flower at S4. (J) Transverse section of a flower at S5. AB, abaxial region of the flower; AD, adaxial region of the flower; c, carpel; l, leaf; o, ovule; p, petal; s, sepal; sp, spur; st, stamen. Black arrowheads point to shoot apical meristems; white arrowheads point to floral primordia. Scale bars = 200 μm.

with a neofunctionalization event. To corroborate this hypothesis, it is critical to investigate in more detail the evolution, function, sequence change and plesiomorphic function of the Tropaeolaceae *TCP4L* genes.

In terms of gene evolution, the duplication that gave rise to the paralogues *TlTCP4L1* and *TlTCP4L2* is shared by *T. longifolium*, *T. majus* and *T. peregrinum*, but not by Akaniaceae species (Fig. 3B). More sampling across Tropaeolaceae will confirm if this *TCP4L* duplication predates Tropaeolaceae diversification and thus coincides with spur evolution (Fig. 3A). This duplication is either specific to this gene lineage, or the result of the whole-genome duplication event suggested for Tropaeolaceae (Lysak, 2018; Mabry *et al*., 2020).

Based on our expression results, *TlTCP4L2* activity during spur initiation could be linked to higher rates of cell division in the adaxial region of the floral tube, as *TlTCP4L2* expression in the nascent spur overlaps with that of *TlHIS4* (Figs 2E and 5F). The role of *CIN3* genes in positively regulating cell division and patterning in the perianth has also been suggested for *Aristolochia* (Pabón-Mora *et al*., 2020) and confirmed in *Antirrhinum* (Crawford *et al*., 2004), as *cin* mutants in the latter have smaller petals and defects in petal epidermis with flat

rather than conical cells (Crawford *et al*., 2004). Conversely, negative regulation of cell division has been attributed to the activity of *CIN3* homologues in spurs of *Aquilegia* (Yant *et al*., 2015) and leaves of *Arabidopsis* and *Antirrhinum* (Nath *et al*., 2003; Palatnik *et al*., 2003; Crawford *et al*., 2004). Available data suggest that *CIN* genes might have contrasting roles in the modulation of cell division (reviewed in Martín-Trillo and Cubas, 2010), and, in the case of *T. longifolium*, it appears predominantly a positive regulation of cell division. It is critical to highlight that *TlTCP4L2* function in spur development must be downstream of factors determining bilateral floral symmetry and floral organ identity. This is based on observations of floral pelorias, with abaxialized flowers lacking spurs, or adaxialized flowers forming five spurs (Dupuy, 1961). Similarly, spurs are also lost in induced homeotic mutants, which exhibit whorls of leaf-like organs instead of floral organs and have tubeless flowers (Kausik, 1938; Astié, 1962; Astié *et al*., 1967).

At later stages of spur development, both *TlTCP4L1* and *TlTCP4L2* could have redundant function in spur elaboration as they are both strongly expressed in the spur. They may not be acting independently. In fact, other Tropaeolaceae *CIN* genes may also have a redundant role in spur elaboration at later stages of development. For instance, *TlTCP2L* (a *CIN1* homologue) and *TlTCP13* (a *CIN2* homologue) have a higher expression in the adaxial tube at S8 according to RT–PCR results (Martínez-Salazar *et al*., 2021). At these later stages, cell division seems to be more dynamic in time and space, as *TlHIS4* expression is initially localized in the outer cell layers (Fig. 2F, G, I), but later it is mostly restricted to the inner ones (Fig. 2L). For spur elaboration, other downstream transcription factors controlling cell expansion and nectary development require further studies; these include the *BES1*/*BRZ1* (*BRI1-EMS-SUPRESSOR1*/*BRASSINAZOLE-RESISTANT1*) and *STYLISH* (*STY*) genes identified in *Aquilegia* (Min *et al*., 2019; Conway *et al*., 2021) and the *YABBY* gene *CRABS CLAW* (*CRC*) identified in *Arabidopsis* (Bowman and Smyth, 1999).

Finally, a role of *CIN3* genes in epidermis development also needs functional validation in Tropaeolaceae. One homologue of these genes in *Arabidopsis*, *TCP4*, is required for epidermal cell differentiation (Vadde *et al*., 2018). Genes that specifically control the acquisition of epidermal cell fate include the HD-ZIP IV genes *Arabidopsis thaliana MERISTEM L1 LAYER* (*ATML1*) and *PROTODERMAL FACTOR2* (*PDF2*) (Lu *et al*., 1996; Abe *et al*., 2003; Javelle *et al*., 2011).

Variations in gene function could be attributed to changes either in coding sequence or in *cis*-regulatory elements. However, even though the coding sequences of the Tropaeolaceae *TCP4L1* and *TCP4L2* differ, their most critical regions are identical. In fact, both Tropaeolaceae and Akaniaceae *TCP4L* genes have an identical *miR319* binding site (5′ AGGGGACCCCUUCAGUCCAGU 3′), which is also identical to that of *Aquilegia TCP4* and *Aristolochia CIN3* (Supplementary Data Fig. S3). The miRNA *miR319* is critical to regulate the translation of *CIN1* and *CIN3* genes (Palatnik *et al*., 2003). Additionally, Tropaeolaceae TCP4L1 and TCP4L2 proteins have a conserved VDWLI motif, which is also identical to that of all other CIN3 proteins sampled (Supplementary Data Figs S3 and S4). This motif is part of the bHLH domain and is crucial for protein interactions (Cubas *et al*., 1999*a*). In contrast to differences in the coding sequence, differences in *cis*-regulatory elements appear as a more likely explanation for the possible functional divergence of the Tropaeolaceae *TCP4L* paralogues. Genome-level data from Tropaeolaceae will be critical to explore these differences.

Assessing the plesiomorphic function of the Tropaeolaceae *TCP4L* genes will require the exploration of their function in closely related taxa, especially in their sister group Akaniaceae. Akaniaceae comprises two spurless species, *Akania bidwillii* and *Bretschneidera sinensis*. The transcriptome of *A. bidwillii* (Carpenter *et al*., 2019; One Thousand Plant Transcriptomes Initiative, 2019) and the published genomes of *B. sinensis* (Liu *et al*., 2022; Zhang *et al*., 2022) allowed us to report that Akaniaceae have an independent duplication of *TCP4L* genes that is not shared with Tropaeolaceae (Fig. 3). This may be the result of a recent whole-genome duplication event reported for *B. sinensis* (Zhang *et al*., 2022). Understanding the function and expression patterns of Akaniaceae *TCP4L* genes and of the homologues in other Brassicales would allow us to hypothesize plesiomorphic functions of this gene lineage and hence acquired functions of the Tropaeolaceae *TCP4L2*.

TlTCP12 expression is restricted to early stages of flower development

We described the detailed spatio-temporal expression of *TlTCP12*, which had been first identified as a late abaxial-associated factor in the floral tube (Martínez-Salazar *et al*., 2021). We observed that this gene is strongly expressed in floral organ primordia at early stages of development, but its broad expression contracts before spur initiation (Fig. 6) into the centre of the flower, where stamen and carpel primordia are located. The specific expression analysis of this gene indicates that it is not actively expressed in the spur (Fig. 6F) and suggests that the RT–PCR sample from the abaxial tube, which is smaller and thus more difficult to dissect than the adaxial tube, incorporated a significant proportion of tissue from the centre of the flower.

As a *CYC* homologue (specifically a *CYC3* homologue), *TlTCP12* was a candidate for the establishment of early bilateral symmetry in Tropaeolaceae flowers. However, genes different from *TCP12* must be determining the adaxial–abaxial differential perianth growth in Tropaeolaceae. Horticultural peloria of *Tropaeolum majus* develop abaxialized flowers that exhibit five sepals and five petals with an abaxial morphology and a radially symmetrical floral tube without spurs (Dupuy, 1961; Comba *et al*., 1999). Additionally, experimentally induced peloria of *T. majus* develop flowers with five sepals and five petals with an adaxial morphology and a radially symmetrical floral tube with five spurs (Dupuy, 1961). Comparative transcriptomics at very early stages of development between adaxial and abaxial flower regions will allow the identification of novel candidate genes involved in the establishment of bilateral floral symmetry in Tropaeolaceae. Alternatively, detailed expression analysis at early stages of development by *in situ* hybridization or functional analysis of *TlTCP1*, the canonical core eudicot *CYC* homologue, will confirm or rule out its function in the independent acquisition of bilateral floral symmetry prior to Tropaeolaceae diversification (Reyes *et al*., 2016). In fact, orthologues of *TlTCP1* in other taxa of Brassicales have

been associated with their independent acquisition of bilateral floral symmetry (Busch and Zachgo, 2007; Busch *et al.*, 2012; Mankowski, 2013).

TlSTM1 and *TlSTM2* have overlapping expression in undifferentiated floral tissues

We detected overlapping expression patterns for *TlSTM1* and *TlSTM2*, which are the result of a Tropaeolaceae-specific gene duplication event (Supplementary Data Fig. S2). These genes are expressed in undifferentiated floral tissues and their overall expression decreases before spur initiation (Fig. 7F, J). *TlSTM1* was previously characterized as a late abaxially expressed gene in the spurless region of the floral tube (Martínez-Salazar *et al*., 2021). However, using *in situ* hybridization, we did not detect differential expression of any of the two paralogues between the adaxial and abaxial regions of the flower. The specific expression analysis for *TlSTM1* suggests that this transcription factor does not control spur development and, as explained above, that the abaxial tube sample used for RT–PCR included a significant proportion of tissue from the centre of the flower, because it is smaller and thus more difficult to dissect than the adaxial tube sample. In fact, according to RT–PCR results, *TlSTM2*, a gene expressed in the centre of the flower but not in the floral tube, has a weak expression in the adaxial region of the tube as compared with the abaxial counterpart (Martínez-Salazar *et al*., 2021). Therefore, the two *STM* homologues may have a redundant role in maintaining cell indeterminacy during flower development. *STM* genes are known to maintain cell indeterminacy in the shoot apical meristem (Long *et al*., 1996). These results are consistent with those found in *Aquilegia*, where *STM* homologues are not expressed in the spur (Yant *et al*., 2015). In turn, spur development in *Aquilegia* is not interpreted as a result of prolonged indeterminacy, such as in *Linaria* (Box *et al*., 2011), but as a product of organ sculpting through the modulation of cell division.

Conclusions

The detailed spatio-temporal expression patterns of candidate genes for bilateral symmetry and spur formation provide a framework to better understand the development and evolution of nectar spurs in Tropaeolaceae. In a developmental context, we describe transcription factors putatively involved in the determination and elaboration of the spur in Tropaeolaceae flowers. We show overlapping expression of the class I *KNOX* genes *TlSTM1* and *TlSTM2* in flower meristems, consistent with a conserved function in meristematic cell identity. We rule out the role of the *CYC3* gene *TlTCP12* in the early establishment of floral bilateral symmetry and suggest the recruitment of other factors that control zygomorphy in Tropaeolaceae flowers. Remarkably, we observe strong expression of the *CIN3* gene *TlTCP4L2*, which overlaps with the marker of cell division *TlHIS4* in the adaxial region of the early floral tube, corresponding to the nascent spur. The same overlapping expression of *CIN3* genes and *TlHIS4* persists in the elongating spur, which suggests a coordinate role for these transcription factors in modulating cell division in this structure. Additionally, high expression of *TlTCP4L2* in the nectariferous tissue of the spur at late developmental stages suggests that the same gene plays a key role in spur elaboration.

In an evolutionary context, families Akaniaceae and Tropaeolaceae (Brassicales) share the presence of a floral tube that lifts the free limbs of sepals and petals. Although there was an independent duplication event of the *TCP4L* genes in each family, only the *TCP4L2* copy in Tropaeolaceae has been likely recruited to function in spur initiation and elaboration. This provides a plausible scenario for neofunctionalization, linked to the formation of nectar spurs in the adaxial region of the floral tube as a fixed trait in Tropaeolaceae.

SUPPLEMENTARY DATA

Supplementary data are available at *Annals of Botany* online and consist of the following. Figure S1: gel electrophoresis of RNA probes and their DNA templates. Figure S2: maximum likelihood analysis of *SHOOT MERISTEMLESS* genes. Gene duplication events are indicated with stars: white star, duplication predating Akaniaceae diversification; red star, duplication predating Tropaeolaceae diversification. Name in orange corresponds to the *A. thaliana* canonical homologue; names in red correspond to the *T. longifolium* homologues *TlSTM1* and *TlSTM2*. Node numbers indicate bootstrap support. Figure S3: fragments of the alignment of *CINCINNATA3* genes, showing the bHLH protein domain and the *miR319* binding site. Figure S4: full protein alignment of Tropaeolaceae and Akaniaceae *CINCINNATA3* genes. Table S1: list of primers used in this study. Table S2: list of names, accession numbers and databases of the sequences used in this study.

FUNDING

This work was supported by Estrategia de Sostenibilidad 2018–2019 from the Universidad de Antioquia and the 2022 Bill Dahl Graduate Student Research Award from the Botanical Society of America.

ACKNOWLEDGEMENTS

We thank the late Dr Jean Paul Delgado (Universidad de Antioquia) for the use of laboratory facilities. We also thank Yesenia Madrigal (Universidad de Antioquia) and Pablo Pérez-Mesa (Universidad Nacional de Colombia) for assistance during laboratory and field work, and two anonymous referees whose comments improved the final version of the manuscript. S.M.-S. and N.P.-M. gathered the experimental data; all authors conceived and designed the study, analysed the results, and wrote and approved the final version of the manuscript.

LITERATURE CITED

Abascal F, **Zardoya R**, **Telford MJ. 2010**. TranslatorX: multiple alignment of nucleotide sequences guided by amino acid translations. *Nucleic Acids Research* **38**: W7–13.

Abe M, **Katsumata H**, **Komeda Y**, **Takahashi T. 2003**. Regulation of shoot epidermal cell differentiation by a pair of homeodomain proteins in *Arabidopsis*. *Development* **130**: 635–643.

Almeida J, **Rocheta M**, **Galego L. 1997**. Genetic control of flower shape in *Antirrhinum majus*. *Development* **124**: 1387–1392.

Andersson L, **Andersson S. 2000**. A molecular phylogeny of Tropaeolaceae and its systematic implications. *Taxon* **49**: 721–736.

Astié M. 1962. Morphoses florales tératologiques induites expérimentalement chez *Tropaeolum majus* L. *Bulletin de la Société Botanique de France* **109**: 115–121.

Astié M, **Coquen CI**, **Debraux G**, **Lecocq M. 1967**. Morphoses tératologiques et virescences florales induites expérimentalement chez quelques angiospermes. *Bulletin de la Société Botanique de France* **114**: 98–108.

Ballerini ES, **Min Y**, **Edwards MB**, **Kramer EM**, **Hodges SA. 2020**. *POPOVICH*, encoding a C2H2 zinc-finger transcription factor, plays a central role in the development of a key innovation, floral nectar spurs, in *Aquilegia*. *Proceedings of the National Academy of Sciences of the USA* **117**: 22552–22560.

Bowman JL, **Smyth DR. 1999**. CRABS CLAW, a gene that regulates carpel and nectary development in *Arabidopsis*, encodes a novel protein with zinc finger and helix-loop-helix domains. *Development* **126**: 2387–2396.

Box MS, **Dodsworth S**, **Rudall PJ**, **Bateman RM**, **Glover BJ. 2011**. Characterization of *Linaria KNOX* genes suggests a role in petal-spur development. *Plant Journal* **68**: 703–714.

Busch A, **Zachgo S. 2007**. Control of corolla monosymmetry in the Brassicaceae *Iberis amara*. *Proceedings of the National Academy of Sciences of the USA* **104**: 16714–16719.

Busch A, **Horn S**, **Mühlhausen A**, **Mummenhoff K**, **Zachgo S. 2012**. Corolla monosymmetry: evolution of a morphological novelty in the Brassicaceae family. *Molecular Biology and Evolution* **29**: 1241–1254.

Carpenter EJ, **Matasci N**, **Ayyampalayam S**, ***et al***. **2019**. Access to RNA-sequencing data from 1,173 plant species: The 1000 Plant transcriptomes initiative (1KP). *GigaScience* **8**: 1–7.

Comba L, **Corbert SA**, **Barron A**, ***et al***. **1999**. Garden flowers: insect visits and the floral reward of horticulturally-modified variants. *Annals of Botany* **83**: 73–86.

Conway SJ, **Walcher-Chevillet CL**, **Barbour KS**, **Kramer EM. 2021**. Brassinosteroids regulate petal spur length in *Aquilegia* by controlling cell elongation. *Annals of Botany* **128**: 931–942.

Corley SB, **Carpentier R**, **Copsey L**, **Coen E. 2005**. Floral asymmetry involves an interplay between TCP and MYB transcription factors in *Antirrhinum*. *Proceedings of the National Academy of Sciences of the USA* **102**: 5068–5073.

Crawford BCW, **Nath U**, **Carpenter R**, **Coen ES. 2004**. *CINCINNATA* controls both cell differentiation and growth in petal lobes and leaves of *Antirrhinum*. *Plant Physiology* **135**: 244–253.

Cubas P, **Lauter N**, **Doebley J**, **Coen E. 1999***a*. The TCP domain: a motif found in proteins regulating plant growth and development. *Plant Journal* **18**: 215–222.

Cubas P, **Vicent C**, **Coen E. 1999***b*. An epigenetic mutation responsible for natural variation in floral symmetry. *Nature* **401**: 157–161.

Dupuy P. 1961. Remarques sur la formation de pièces anormales dans le périanthe des fleurs de *Tropaeolum majus* L. et *Linaria spuria* Mill, au cours de l'induction expérimentale de la pélorie par l'acide 2,4-dichlorophénoxyacétique. *Bulletin de la Société Botanique de France* **108**: 375–387.

Dupuy L, **Mackenzie J**, **Haseloff J. 2010**. Coordination of plant cell division and expansion in a simple morphogenetic system. *Proceedings of the National Academy of Sciences of the USA* **107**: 2711–2716.

Ferrándiz C, **Gu Q**, **Martienssen R**, **Yanofsky F. 2000**. Redundant regulation of meristem identity and plant architecture by *FRUITFULL*, *APETALA1* and *CAULIFLOWER*. *Development* **127**: 725–734.

Golz JF, **Keck EJ**, **Hudson A. 2002**. Spontaneous mutations in *KNOX* genes give rise to a novel floral structure in *Antirrhinum*. *Current Biology* **12**: 515–522.

Hodges SA. 1997. Floral nectar spurs and diversification. *International Journal of Plant Sciences* **158**: S81–S88.

Hodges SA, **Arnold ML. 1995**. Spurring plant diversification: are floral nectar spurs a key innovation? *Proceedings of the Royal Society B* **262**: 343–348.

Javelle M, **Vernoud V**, **Rogowsky PM**, **Ingram GC. 2011**. Epidermis: the formation and functions of a fundamental plant tissue. *New Phytologist* **189**: 17–39.

Kausik SB. 1938. Morphology of abnormal flowers in some angiosperms. *New Phytologist* **37**: 396–408.

Letunic I, **Bork P. 2019**. Interactive Tree Of Life (iTOL) v4: recent updates and new developments. *Nucleic Acids Research* **47**: W256–W259.

Liu HL, **Harris AJ**, **Wang ZF**, **Chen HF**, **Li ZA**, **Wei X. 2022**. The genome of the Paleogene relic tree *Bretschneidera sinensis*: insights into trade-offs in gene family evolution, demographic history, and adaptive SNPs. *DNA Research* **29**: 1–15.

Long JA, **Moan EI**, **Medford JI**, **Barton MK. 1996**. A member of the KNOTTED class of homeodomain proteins encoded by the *STM* gene of *Arabidopsis*. *Nature* **379**: 66–69.

Lu P, **Porat R**, **Nadeau JA**, **O'Neil SD. 1996**. Identification of a meristem L1 layer-specific gene in *Arabidopsis* that is expressed during embryonic pattern formation and defines a new class of homeobox genes. *Plant Cell* **8**: 2155–2168.

Luo D, **Carpenter R**, **Vincent C**, **Copsey L**, **Coen E. 1996**. Origin of floral asymmetry in *Antirrhinum*. *Nature* **383**: 794–799.

Lysak MA. 2018. Brassicales: an update on chromosomal evolution and ancient polyploidy. *Plant Systematics and Evolution* **304**: 757–762.

Mabry ME, **Brose JM**, **Blischak PD**, ***et al***. **2020**. Phylogeny and multiple independent whole-genome duplication events in the Brassicales. *American Journal of Botany* **107**: 1148–1164.

Mankowski PJ. 2013. *A functional approach to profiling candidate genes in non model Brassicales*. Master's Thesis, University of Alberta, Canada.

Martínez-Salazar S, **González F**, **Alzate JF**, **Pabón-Mora N. 2021**. Molecular framework underlying floral bilateral symmetry and nectar spur development in *Tropaeolum*, an atypical member of the Brassicales. *American Journal of Botany* **108**: 1315–1330.

Martín-Trillo M, **Cubas P. 2010**. TCP genes: a family snapshot ten years later. *Trends in Plant Science* **15**: 31–39.

Min Y, **Bunn I**, **Kramer EM. 2019**. Homologs of the *STYLISH* gene family control nectary development in *Aquilegia*. *New Phytologist* **221**: 1090–1100.

Nath U, **Crawford BCW**, **Carpenter R**, **Coen E. 2003**. Genetic control of surface curvature. *Science* **299**: 1404–1407.

One Thousand Plant Transcriptomes Initiative. **2019**. One thousand plant transcriptomes and the phylogenomics of green plants. *Nature* **574**: 679–685.

Pabón-Mora N, **Madrigal Y**, **Alzate JF**, ***et al***. **2020**. Evolution of Class II *TCP* genes in perianth bearing Piperales and their contribution to the bilateral calyx in *Aristolochia*. *New Phytologist* **228**: 752–769.

Palatnik JF, **Allen E**, **Wu X**, ***et al***. **2003**. Control of leaf morphogenesis by microRNAs. *Nature* **425**: 257–263.

Rebocho AB, **Southman P**, **Kennaway JR**, **Bangham JA**, **Coen E. 2017**. Generation of shape complexity through tissue conflict resolution. *eLife* **6**: e20156.

Reyes E, **Sauquet H**, **Nadot S. 2016**. Perianth symmetry changed at least 199 times in angiosperm evolution. *Taxon* **65**: 945–964.

Ronse De Craene LP, **Smets EF. 2001**. Floral developmental evidence for the systematic relationships of *Tropaeolum* (Tropaeolaceae). *Annals of Botany* **88**: 879–892.

Ronse De Craene LP, **Yang TYA**, **Schols P**, **Smets EF. 2002**. Floral anatomy and systematics of *Bretschneidera* (Bretschneideraceae). *Botanical Journal of the Linnean Society* **139**: 29–45.

Silvestro D, **Michalak I. 2012**. raxmlGUI: a graphical front-end for RAxML. *Organisms, Diversity & Evolution* **12**: 335–337.

Vadde BVL, **Challa KR**, **Nath U. 2018**. The TCP4 transcription factor regulates trichome cell differentiation by directly activating *GLABROUS INFLORESCENCE STEMS* in *Arabidopsis thaliana*. *Plant Journal* **93**: 259–269.

Vlašánková A, **Padyšáková E**, **Bartoš M**, **Mengual X**, **Janečková P**, **Janeček S. 2017**. The nectar spur is not only a simple specialization for long-proboscid pollinators. *New Phytologist* **215**: 1574–1581.

Yant L, **Collani S**, **Puzey J**, **Levy C**, **Kramer EM. 2015**. Molecular basis for three-dimensional elaboration of the *Aquilegia* petal spur. *Proceedings of the Royal Society B* **282**: 20142778.

Zhang H, **Du X**, **Dong C**, ***et al***. **2022**. Genomes and demographic histories of the endangered *Bretschneidera sinensis* (Akaniaceae). *GigaScience* **11**: 1–10.